AEROSPACE REPORT NO.
TR-2014-01128

1-D Heat Transfer in Multilayer Materials Using a Finite Volume Approach

January 1, 2014

Marcus A. Lobbia
Launch Strike and Range
Developmental Planning and Projects

Prepared for:

Space and Missile Systems Center
Air Force Space Command
483 N. Aviation Blvd.
El Segundo, CA 90245-2808

Authorized by: Systems Planning, Engineering, and Quality

The cost to prepare this document: $395

This report was submitted by The Aerospace Corporation, El Segundo, CA 90245-4691, under Contract No. FA8802-09-C-0001 with the Space and Missile Systems Center, 483 N. Aviation Blvd., El Segundo, CA 90245. It was reviewed and approved for The Aerospace Corporation by Joseph D. Adams, systems director, Launch Strike and Range. Capt. Brian E. Donegan was the project officer for the Development Planning (XR) program.

Approval on File

Capt. Brian E. Donegan
SMC/XR

REPORT DOCUMENTATION PAGE

Form Approved
OMB No. 0704-0188

1. REPORT DATE (*DD-MM-YYYY*)	**2. REPORT TYPE**	**3. DATES COVERED *(From - To)***
01-01-2014		

4. TITLE AND SUBTITLE

1-D Heat Transfer in Multilayer Materials Using a Finite Volume Approach

5a. CONTRACT NUMBER
FA8802-09-C-0001

5b. GRANT NUMBER

5c. PROGRAM ELEMENT NUMBER

6. AUTHOR(S)

Marcus A. Lobbia

5d. PROJECT NUMBER

5e. TASK NUMBER

5f. WORK UNIT NUMBER

7. PERFORMING ORGANIZATION NAME(S) AND ADDRESS(ES)

The Aerospace Corporation
Developmental Planning and Projects
El Segundo, CA 90245-4691

8. PERFORMING ORGANIZATION REPORT NUMBER

TR-2014-01128

9. SPONSORING/MONITORING AGENCY NAME(S) AND ADDRESS(ES)

Space and Missile Systems Center
Air Force Space Command
483 N. Aviation Blvd.
El Segundo, CA 90245

10. SPONSOR/MONITOR'S ACRONYM(S)
SMC

11. SPONSOR/MONITOR'S REPORT NUMBER(S)

12. DISTRIBUTION/AVAILABILITY STATEMENT

Approved for public release; distribution unlimited.

13. SUPPLEMENTARY NOTES

14. ABSTRACT

One-dimensional transient heat transfer analysis is frequently used to provide quick estimates of the performance of thermal protection system concepts for reentry systems. While finite difference techniques are commonly employed when solving simple single-material thermal problems, more complex cases with multiple layers can complicate the numerical implementation. A control volume analysis is used in the present work to derive a finite volume approach to the 1-D thermal analysis problem using generalized coordinates. Details of the numerical implementation are also discussed to highlight how this technique can simplify the overall solution process. Finally, two example problems are used to validate the accuracy of the approach, one of which involves analysis of a multilayer TPS problem with non-uniform grid spacing.

15. SUBJECT TERMS

Heat Transfer, Multilayer Thermal Analysis, Finite Volume, Generalized Coordinates

16. SECURITY CLASSIFICATION OF:			**17. LIMITATION OF ABSTRACT**	**18. NUMBER OF PAGES**	**19a. NAME OF RESPONSIBLE PERSON**
					Marcus A. Lobbia
a. REPORT	**b. ABSTRACT**	**c. THIS PAGE**		22	**19b. TELEPHONE NUMBER**
UNCLASSIFIED	**UNCLASSIFIED**	**UNCLASSIFIED**			310-336-2709

Abstract

One-dimensional transient heat transfer analysis is frequently used to provide quick estimates of the performance of thermal protection system concepts for reentry systems. While finite difference techniques are commonly employed when solving simple single-material thermal problems, more complex cases with multiple layers can complicate the numerical implementation. A control volume analysis is used in the present work to derive a finite volume approach to the 1-D thermal analysis problem using generalized coordinates. Details of the numerical implementation are also discussed to highlight how this technique can simplify the overall solution process. Finally, two example problems are used to validate the accuracy of the approach, one of which involves analysis of a multilayer TPS problem with non-uniform grid spacing.

Contents

Figures

Tables

Nomenclature

α	= thermal diffusivity
ε	= emissivity
ρ	= density
σ	= Stefan-Boltzman constant
θ	= time integration weighting factor
ξ	= spatial coordinate, computational plane
c_p	= heat capacity
$\dot{E}$	= energy rate with respect to time
$\vec{F}$	= directional heat flux vector
Fo	= Fourier number
k	= thermal conductivity
$\vec{n}$	= surface normal vector
q	= heat flux (per unit area)
q_g	= heat generation rate (per unit volume)
S	= surface area
T	= temperature
t	= time
u	= generic property in a control volume
V	= volume
x	= spatial coordinate, physical plane

Subscripts/Superscripts

cond	= conduction
conv	= convection
g	= internal generation
j	= grid index
L	= left side
n	= time index
R	= right side
rad	= radiation
x	= derivative with respect to spatial coordinate *x*

1. Introduction

The solution of the transient one-dimensional heat diffusion equation is an elementary problem taught in many courses on heat transfer. While exact solutions are possible for a subset of problems, engineering applications typically involve using numerical techniques to obtain an approximate solution to the heat equation. For a simple analysis involving a single material with uniform grid spacing, finite difference methods are straightforward. For more complex engineering problems where the computational grid spacing is not uniform, and/or where different materials are being considered (i.e. composite slabs), it will be shown that the implementation of a finite volume technique using a generalized (i.e. curvilinear) coordinate transformation can help simplify the numerical approach.

Although several authors have published material discussing the numerical solution of the heat diffusion equation using finite volume techniques [1] or two-dimensional generalized coordinates [2], and industry standard thermal analysis tools such as FIAT [3] use a finite volume solution technique, the author is unaware of a reference describing the derivation and finite volume numerical implementation of the transient one-dimensional heat diffusion equation using generalized coordinates. The present work is therefore aimed at addressing this, as well as presenting an example of an engineering application of the technique for multi-material composite slabs.

2. Finite Volume Formulation Using Generalized Coordinates

A finite volume approach is an intuitive technique that can be associated with the control volume analysis that can be used to derive the heat diffusion equation. In this approach, the quantities of interest in a given control volume are typically defined as a *de facto* averaged value. For example, consider a variable $u(x, y, z)$ that varies as a function of location within a three-dimensional control volume. The "averaged" value of u can be found by integrating the function over the entire volume:

$$\int_V u\, dV = \overline{u}\, V \tag{1}$$

where $\overline{u}$ represents the averaged value of u.

To apply this approach to the heat diffusion equation, first consider an energy rate balance for a control volume, which can be written assuming conservation of energy as

$$\dot{E}_{stored} = \dot{E}_{cond} + \dot{E}_{conv} + \dot{E}_{rad} + \dot{E}_g \tag{2}$$

In equation (2), the rate of energy stored in the control volume ($\dot{E}_{stored}$) is equal to the net energy rates into the control volume due to conduction ($\dot{E}_{cond}$), convection ($\dot{E}_{conv}$), radation ($\dot{E}_{rad}$), and internal energy generation ($\dot{E}_g$). The rate of energy stored can be written as

$$\dot{E}_{stored} = \frac{\partial}{\partial t}\int_V \rho c_p\, T dV = \int_V \rho c_p \frac{\partial T}{\partial t} dV = \left(\bar{\rho}\bar{c_p}\frac{\partial \overline{T}}{\partial t}\right)V \tag{3}$$

where V represents the size of the control volume. The term $\bar{\rho}\bar{c_p}(\partial\bar{T}/\partial t)$ is the change with respect to time of thermal energy in the material per unit volume, with the overbars on the variables denoting "averaged" values for the control volume as defined previously. Note that in equation (3), it is assumed that the material density and specific heat do not change over the time interval being evaluated.

The net energy rates due to conduction, convection, and radiation can be represented by integrating the net heat flux entering the control volume due to the appropriate physical phenomena. For example, the net energy rate due to conduction can be written as

$$\dot{E}_{cond} = \int_S \vec{F}_{cond} \cdot \vec{n}\, dS \tag{4}$$

where $\vec{F}_{cond}$ represents the directional heat flux due to conduction, $\vec{n}$ is the outward pointing surface normal, and S represents the total surface area of the control volume. Similar equations can be written for the convective and radiative net energy rates.

Finally, the net change in energy due to internal heat generation can be written as the averaged value of the heat generation rate per unit volume multiplied by the control volume size:

$$\dot{E}_g = \int_V q_g\ dV = \overline{q_g}V \tag{5}$$

Using equations (3)-(5), the conservation law defined in equation (2) can be rewritten in integral form for the control volume as

$$\frac{\partial}{\partial t}\int_V \rho c_p\, T dV = \int_S \vec{F}_{cond} \cdot \vec{n}\, dS + \int_S \vec{F}_{conv} \cdot \vec{n}\, dS + \int_S \vec{F}_{rad} \cdot \vec{n}\, dS + \int_V q_g\ dV \tag{6}$$

In the case of a one-dimensional control volume, the volume reduces to a length Δx, and the surface area reduces to unity; therefore equation (6) can then be rewritten as

$$\left(\bar{\rho}\bar{c_p}\frac{\partial\bar{\bar{T}}}{\partial t}\right)\Delta x = \left(F_{cond_{in}} - F_{cond_{out}}\right) + \left(F_{conv_{in}} - F_{conv_{out}}\right) + \left(F_{rad_{in}} - F_{rad_{out}}\right) + \overline{q_g}\Delta x \tag{7}$$

where the subscripts in and out refer to the conductive, convective, and radiative heat fluxes into and out of the control volume in the x-direction.

Using Fourier's law for conductive heat transfer, equation (7) can then be rewritten as

$$\left(\bar{\rho}\bar{c_p}\frac{\partial\bar{\bar{T}}}{\partial t}\right)\Delta x = \left[\left(-k\frac{\partial T}{\partial x}\right)\Big|_{in} - \left(-k\frac{\partial T}{\partial x}\right)\Big|_{out}\right] + \left(F_{conv_{in}} - F_{conv_{out}}\right) + \left(F_{rad_{in}} - F_{rad_{out}}\right) + \overline{q_g}\Delta x \tag{8}$$

where the derivative $\partial T/\partial x$ in equation (8) is evaluated at the control volume interfaces.

Non-uniform spacing of the finite volume cells can complicate the implementation of numerical approaches to solving Equation (8). Therefore, a coordinate transformation can be applied using a generalized coordinate $\xi(x)$ that is a known function of x; typically the transformation is defined such that $\xi(x)$ has uniform spacing to simplify the numerical analysis. Applying the chain rule of differentiation, Equation (8) can be converted to generalized coordinates as

$$\left(\bar{\rho}\bar{c_p}\frac{\partial \bar{T}}{\partial t}\right)\Delta x = \left[\left(-k\frac{d\xi}{dx}\frac{\partial T}{\partial \xi}\right)\Big|_{in} - \left(-k\frac{d\xi}{dx}\frac{\partial T}{\partial \xi}\right)\Big|_{out}\right] + \left(F_{conv_{in}} - F_{conv_{out}}\right) + \left(F_{rad_{in}} - F_{rad_{out}}\right) + \overline{q_g}\Delta x \tag{9}$$

3. Numerical Implementation

The previous section discussed the derivation of the one-dimensional heat diffusion equation using a control volume approach. From a numerical standpoint, this can be thought of as equivalent to a cell-centered finite volume approach, where the center of each cell is assigned an integer index value j, and the cell interfaces have a fractional (e.g. $j \pm 1/2$) index.

In the solution of equation (9), the coordinate transformation is defined such that $\xi(x)$ has uniform spacing of $\Delta\xi = 1$. The grid transformation metrics in equation (9) can be numerically approximated at the cell center as

$$\xi_{x_j} = \frac{d\xi}{dx}\Big|_j = \frac{\xi_{j+1/2} - \xi_{j-1/2}}{x_{j+1/2} - x_{j-1/2}} = \frac{1}{x_{j+1/2} - x_{j-1/2}} = \frac{1}{\Delta x_j} \tag{10}$$

Likewise, the grid metrics at the cell interfaces can approximated numerically in a similar fashion:

$$\begin{aligned} \xi_{x_{j-1/2}} &= \frac{d\xi}{dx}\Big|_{j-1/2} = \frac{\xi_j - \xi_{j-1}}{x_j - x_{j-1}} = \frac{1}{x_j - x_{j-1}} \\ \xi_{x_{j+1/2}} &= \frac{d\xi}{dx}\Big|_{j+1/2} = \frac{\xi_{j+1} - \xi_j}{x_{j+1} - x_j} = \frac{1}{x_{j+1} - x_j} \end{aligned} \tag{11}$$

For the remainder of the discussion in this section, the convective and radiative heat fluxes are assumed to be zero, as these are typically incorporated into the boundary conditions for many engineering problems of interest. Additionally, the internal heat generation term is assumed to be zero (i.e. no heat sources exist in the material). Equation (9) can then be rewritten for a computational cell with index j as

$$\left(\bar{\rho}\bar{c_p}\frac{\partial \bar{T}}{\partial t}\right)\Big|_j \Delta x_j = \left[\left(-k\xi_x\frac{\partial T}{\partial \xi}\right)\Big|_{j-1/2} - \left(-k\xi_x\frac{\partial T}{\partial \xi}\right)\Big|_{j+1/2}\right] \tag{12}$$

The time derivative can be approximated numerically using a first order backwards difference; the conductive heat fluxes at the cell interfaces can be constructed numerically based on the temperature in the cells on each side of the interface. This allows equation (12) to be written as

$$\left(\rho_j c_{p_j} \frac{T_j^n - T_j^{n-1}}{\Delta t}\right)\Delta x_j$$
$$= (1-\theta)\left(k_{j+\frac{1}{2}}\xi_{x_{j+\frac{1}{2}}} \frac{T_{j+1}^{n-1} - T_j^{n-1}}{\Delta\xi} - k_{j-\frac{1}{2}}\xi_{x_{j-\frac{1}{2}}} \frac{T_j^{n-1} - T_{j-1}^{n-1}}{\Delta\xi}\right) \quad (13)$$
$$+ \theta\left(k_{j+\frac{1}{2}}\xi_{x_{j+\frac{1}{2}}} \frac{T_{j+1}^{n} - T_j^{n}}{\Delta\xi} - k_{j-\frac{1}{2}}\xi_{x_{j-\frac{1}{2}}} \frac{T_j^{n} - T_{j-1}^{n}}{\Delta\xi}\right)$$

where n refers to the current time step in a numerical integration, and $n-1$ corresponds to the previous time step. The weighting factor θ is defined between 0 and 1, where $\theta = 0$ represents an explicit time integration approach, and $\theta = 1$ is fully implicit.

Note that the material density and heat capacity in equation (13) are defined at the cell center j, whereas the thermal conductivity is defined at the cell interfaces $j \pm 1/2$. One may be tempted to use an arithmetic mean to determine the thermal conductivity at the cell interfaces. Patankar [1], however, has shown that this can lead to incorrect results when analyzing composite slabs with abrupt changes in the thermal conductivity between materials, and that a better approach is to consider a control volume between the cell centers of the two cells adjoining the interface as a composite slab, and apply a steady-state one-dimensional heat conduction analysis. Assuming that the cell interfaces are midway between the cell centers, this analysis simplifies such that the interface thermal conductivity is the harmonic mean of the thermal conductivities in the two cells adjoining the interface, which can be written as

$$k_{x_{j\pm1/2}} = \frac{2k_j k_{j\pm1}}{k_j + k_{j\pm1}} \quad (14)$$

Due to the fact that the coordinate transformation is defined such that $\Delta\xi = 1$, and noting from equation (10) that $\Delta x_j = 1/\xi_{x_j}$ for a given cell with index j, rearranging and simplifying terms allows equation (13) to be rewritten for an explicit integration scheme with $\theta = 0$ as

$$T_j^n = T_j^{n-1} + \frac{\Delta t}{\rho_j c_{p_j}} \xi_{x_j}\left[k_{j+1/2}\xi_{x_{j+1/2}}\left(T_{j+1}^{n-1} - T_j^{n-1}\right) - k_{j-1/2}\xi_{x_{j-1/2}}\left(T_j^{n-1} - T_{j-1}^{n-1}\right)\right] \quad (15)$$

The explicit integration scheme shown in equation (14) is a simple function of the temperature distribution at the previous time step, but the Fourier number must be less than or equal to 0.5 (for a one-dimensional analysis) to maintain numerical stability [4], where the Fourier number is defined as

$$Fo = \frac{\alpha(\Delta t)}{(\Delta x)^2} = \frac{k_j(\Delta t)}{\rho_j c_{p_j}}\left(\xi_{x_j}\right)^2 \quad (16)$$

Depending on the specific problem being analyzed, the thermal diffusivity may be a function of temperature and location in a multi-material composite slab, and the spacing in the x-direction may not be uniform. Therefore, for an explicit analysis, the stability constraint should be evaluated on a per-cell, per-time step basis to determine the maximum time step possible in the integration of equation (15).

For an implicit time integration technique with $\theta = 1$, equation (13) can similarly be simplified to

$$T_{j-1}^{n}\left[-k_{j-1/2}\xi_{x\,j-1/2}\left(\frac{\Delta t}{\rho_j c_{p_j}}\xi_{x\,j}\right)\right] + T_j^n\left[1 + \left(k_{j+1/2}\xi_{x\,j+1/2} + k_{j-1/2}\xi_{x\,j-1/2}\right)\left(\frac{\Delta t}{\rho_j c_{p_j}}\xi_{x\,j}\right)\right] + T_{j+1}^{n}\left[-k_{j+1/2}\xi_{x\,j+1/2}\left(\frac{\Delta t}{\rho_j c_{p_j}}\xi_{x\,j}\right)\right] = T_j^{n-1} \tag{17}$$

Note that equation (17) is a linear system of equations that must be solved simultaneously to update the temperature for time step n, but has no numerical stability limitations on the time step size. Equation (17) results in a tridiagonal matrix of coefficients for the system of equations, which can be solved efficiently using standard inversion techniques such as the Thomas algorithm.

4. Calculation of Cell Interface Temperatures and Boundary Conditions

While the finite volume approach discussed above makes intuitive use of control volume analysis to derive a numerical solution technique, one challenging aspect lies in the way the boundary conditions are implemented. As the material being analyzed is discretized into finite volume cells to solve equation (15) or (17), the cell-centered approach discussed means that the temperature is updated at the cell centers. The question then arises as to how to determine the temperature at the interfaces between cells, as the edges of the material (which are cell interfaces) are typically prime areas of interest in an engineering analysis.

Similar to the discussion of calculating the cell interface thermal conductivity, the use of steady-state one-dimensional heat conduction is useful. Consider the control volume shown in Figure 1, where the boundaries of the control volume correspond to locations halfway between a finite volume cell interface and the centers of the two finite volume cells adjoining the interface. A steady-state one-dimensional heat conduction equation can be written for this control volume similar to equation (12), except that the left hand side of the equation is set to zero due to the steady-state assumption, and the fluxes are constructed numerically taking into account that the control volume is half the size of a normal finite volume cell:

$$\left(-k\xi_x\frac{\partial T}{\partial \xi}\right)\Big|_L - \left(-k\xi_x\frac{\partial T}{\partial \xi}\right)\Big|_R = 0 \tag{18}$$

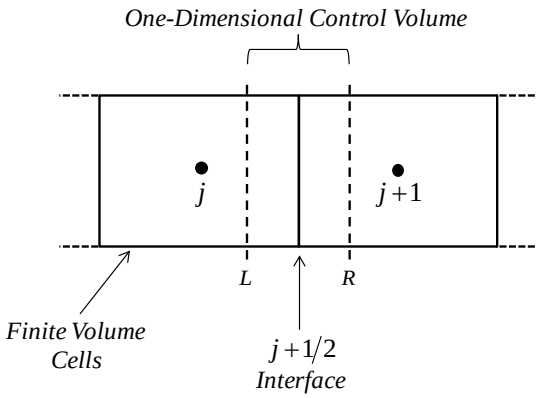

Figure 1. Depiction of a one-dimensional control volume used to determine the temperature at the cell interfaces.

Again approximating the derivatives numerically, this reduces to

$$k_R \xi_{x_R} \frac{T_{j+1} - T_{j+1/2}}{\Delta\xi/2} - k_L \xi_{x_L} \frac{T_{j+1/2} - T_j}{\Delta\xi/2} = 0 \tag{19}$$

As the L and R boundaries of the control volume lie within finite volume cells, the thermal conductivity at the control volume boundaries is assumed to be the "averaged" value in each cell as defined in equation (1). Therefore, equation (19) can be rewritten (dividing out the constant $\Delta\xi/2$ and approximating the grid metrics at the L and R boundaries numerically) as

$$k_{j+1} \xi_{x_{j+1}} \left(T_{j+1} - T_{j+1/2}\right) - k_j \xi_{x_j} \left(T_{j+1/2} - T_j\right) = 0 \tag{20}$$

Finally, rearranging terms then allows the cell interface temperature to be calculated as

$$T_{j+1/2} = \frac{k_{j+1} \xi_{x_{j+1}} T_{j+1} + k_j \xi_{x_j} T_j}{k_{j+1} \xi_{x_{j+1}} + k_j \xi_{x_j}} \tag{21}$$

For TPS-related engineering applications, the problem is typically such that a multilayer TPS material with boundaries on each end is subject to convective heat fluxes (e.g. due to a high temperature flow over the material) and radiative heat fluxes (e.g. when the surface temperature is significant). To apply these types of boundary conditions to the solution of equation (15) or (17), a straightforward technique is to use "ghost" cells that extend past the boundary, as shown in Figure 2. For this example, a steady-state heat flux balance can be written at the boundary wall (index $j = 1/2$) as

$$q_{cond} = q_{conv} + q_{rad} \tag{22}$$

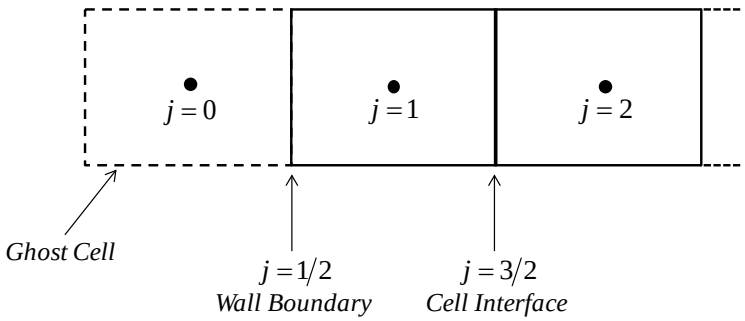

Figure 2. Example of a one-dimensional ghost cell used to apply a wall boundary condition

Using Fourier's law and the Stefan-Boltzmann law, this can be rewritten as

$$\left(-k\xi_x \frac{\partial T}{\partial \xi}\right) = q_{conv} - \sigma\varepsilon T^4 \tag{23}$$

where the variables in equation (23) are evaluated at the boundary wall. Note that while the convective heat flux is typically written in terms of the heat transfer coefficient and difference between the recovery and wall temperatures, for the purposes of the present work it is treated as a "general" heat flux input into the surface that is not dependent on wall temperature. Likewise, for simplicity the temperature of the surroundings used to determine the radiative heat flux is also assumed to be zero in equation (23). Note that while the steady-state heat flux balance used above only considers boundary condition heat fluxes due to conduction, convection, and radiation, other thermodynamic phenomena (e.g. ablation heating or cooling) could be incorporated into equation (22) as appropriate.

Using the indices listed in Figure 2, equation (23) can be rewritten (approximating the spatial derivative numerically and using subscripts to denote the grid indices) as

$$-k_{1/2}\xi_{x_{1/2}}(T_1 - T_0) = q_{conv_{1/2}} - \sigma\varepsilon_{1/2}\left(T_{1/2}\right)^4 \tag{24}$$

Rearranging terms allows the temperature in the ghost cell to be calculated as

$$T_0 = T_1 + \frac{q_{conv_{1/2}} - \sigma\varepsilon_{1/2}\left(T_{1/2}\right)^4}{k_{1/2}\xi_{x_{1/2}}} \tag{25}$$

The ghost cell at $j = 0$ is essentially an "imaginary" mirror image cell used to allow the use of equations (15) or (17) with no special treatment at the boundaries (aside from normal handling of boundary condition values). Therefore it is assumed to be the same size and have the same material properties as the cell at $j = 1$, i.e. the thermal conductivity, emissivity, and grid metrics at the wall are identical to the averaged properties for the cell at $j = 1$ (e.g. $k_{j=1/2} = k_{j=0} = k_{j=1}$). Equation (21) can then be used to calculate the temperature at the wall as

$$T_{1/2} = \frac{k_1 \xi_{x_1} T_1 + k_1 \xi_{x_1} T_0}{k_1 \xi_{x_1} + k_1 \xi_{x_1}} = \frac{T_1 + T_0}{2} \tag{26}$$

In equation (25) the temperature at T_0 is a function of the temperature at $T_{1/2}$ due to the radiative heat flux, yet in equation (26) the temperature at $T_{1/2}$ is a function of T_0. Therefore, in the numerical application of the boundary condition where the radiative heat flux at the wall is non-zero, equations (25) and (26) need to be solved using an iterative technique. While in some cases equations (25) and (26) can be successively iterated until the values of T_0 and $T_{1/2}$ reach a constant value within a specified tolerance, convergence may be slow or difficult to achieve in situations with large temperature gradients and high surface temperatures. The use of a robust root finding technique (such as Brent's algorithm [5]) can eliminate this issue.

The same technique discussed above can be used to derive the boundary condition at the $j = jmax + 1/2$ boundary wall of the grid using a ghost cell at $j = jmax + 1$. This results in

$$T_{jmax+1} = T_{jmax} + \frac{q_{conv\,jmax+1/2} - \sigma \varepsilon_{jmax} \left(T_{jmax+1/2}\right)^4}{k_{jmax+1/2} \xi_{x\,jmax+1/2}} \tag{27}$$

and

$$T_{jmax+1/2} = \frac{T_{jmax+1} + T_{jmax}}{2} \tag{28}$$

which again must be solved using an iterative technique for boundaries with non-zero radiative heat flux until T_{jmax} and $T_{jmax+1/2}$ reach a constant value.

Note that for an implicit time integration technique, equations (25) and (27) supplement the linear system described in equation (17) to provide equations for the temperature at the boundaries.

5. Validation and Example Cases

To assess the validity of the solution technique described above, a thermal analysis tool was created in Excel using Visual Basic for Applications. A simple validation case was run considering a problem in which a semi-infinite slab of copper (k = 401 W/m*K, α =1.17x10^{-4} m^2/s) at an initial uniform temperature of $T_{initial}$ =20 ℃ is exposed to a constant net heat flux input of q_{net} = 3x10^5 W/m^2 on one side. This problem is identical to Example 5.8 described in Ref. [4], which notes that the analytical solution for $T(x,t)$ at a given time t and location x from the wall can be written as

$$T(x,t) = T_{initial} + \frac{2q_{net}\sqrt{\alpha t/\pi}}{k} \exp\left(-\frac{x^2}{4\alpha t}\right) - \frac{q_{net} x}{k} erfc\left(\frac{x}{2\sqrt{\alpha t}}\right) \tag{29}$$

The finite volume method discussed in the present work was used to solve the one-dimensional unsteady heat diffusion equation in the copper slab, where q_{net} is assumed to be equivalent to $q_{conv} + q_{rad}$ in equation (22). For the purposes of this analysis, the results from the

explicit algorithm shown in equation (15) were compared to the analytical solution defined above, as well as to the explicit finite-difference algorithm results listed in Ref. [4]. This comparison was performed for the case where Fo=0.25 and Δx=75 mm, which results in Δt=12 s. The results obtained by solving equation (15) for the first 9 cell interfaces of the finite volume cells nearest the wall are identical to that listed in Ref. [4] for the finite difference solution on 9 nodes (located at the same x locations as the finite volume cell interfaces). Finally, Figure 3 plots the temperature distribution in the material at t=120 s as a function of distance from the wall. As can be observed, the finite volume solution is equal to the finite difference solution, and both are reasonable approximations to the analytical results obtained by equation (29).

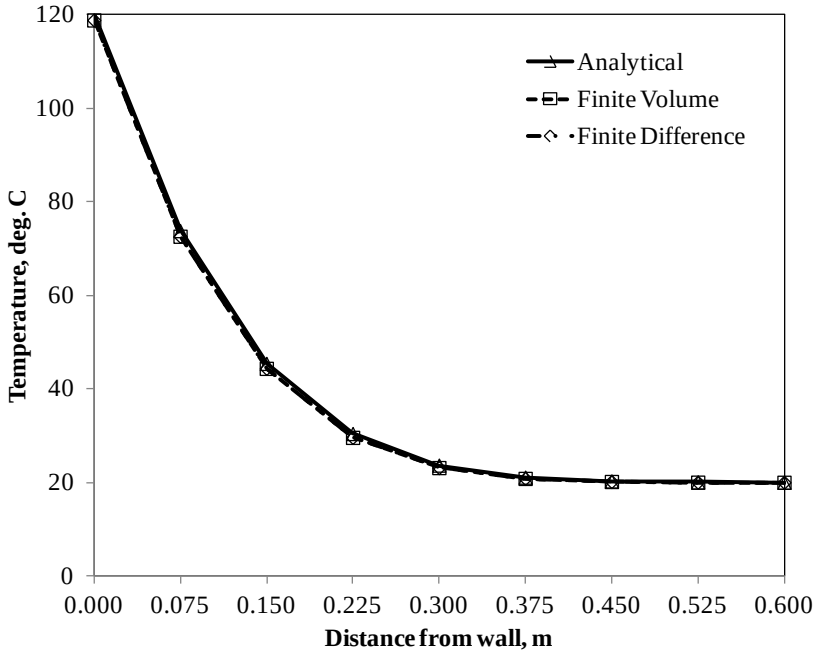

Figure 3. Temperature distribution in copper slab example at time t=120 s.

While the validation case above demonstrates that the finite volume formulation can produce results equivalent to those generated using a node-centered finite difference approach, the primary benefit of the technique described in the present work is in the application to more complex engineering problems involving multi-material composite slabs and non-uniform grid spacing. Consider the example of a gliding reentry vehicle with a thermal protection system (TPS) configuration consisting of the materials shown in Table 1. A thermal analysis can be conducted to assess the temperatures in the material as the reentry vehicle is subjected to the heat flux indicated in Figure 4. For this purpose, the implicit version of the finite volume technique described in the present work was used; the same example was also run with the industry standard thermal analysis program FIAT [3] to confirm the results. Both analyses used the same material properties, outer boundary heat flux input show in Figure 4, and an adiabatic inner boundary condition. At the outer boundary, the radiative heat flux was also included (which required an iterative solution of (25) and (26) as discussed in Section 4).

Table 1. Materials in TPS Composite Slab Example

Layer	Material	Thickness, cm
Outer Layer	Carbon-Carbon	1.27
Interior Layer	Carbon Felt	0.95
Interior Layer	Min-K Insulation	4.57
Inner Layer	Titanium	1.27

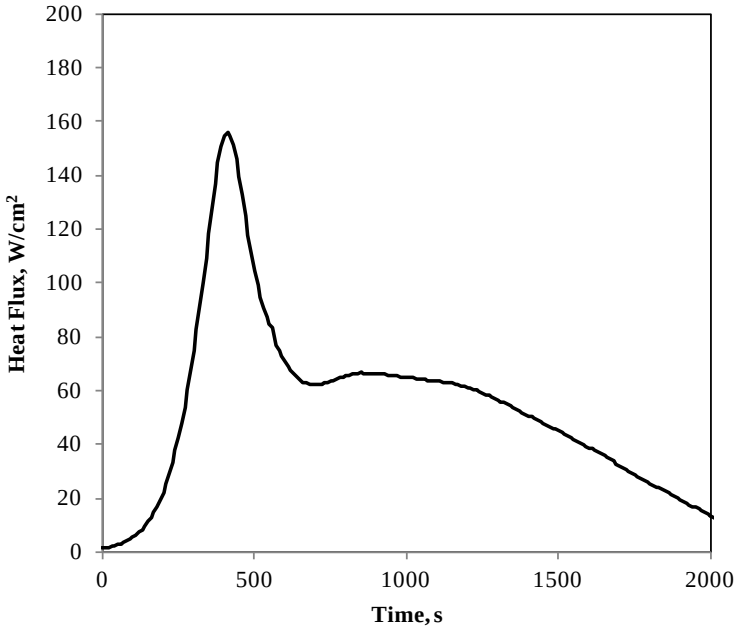

Figure 4. Heat flux input to outer boundary for TPS composite slab example.

The outer and inner boundary temperature time history for this TPS composite slab example is compared in Figure 5; it can be seen that the results from FIAT are essentially identical to those of the present work. (For the FIAT analysis, the default option of having FIAT generate the computational grid was used; this resulted in 64 grid points for FIAT vs. the 23 cells used in the finite volume results shown in Figure 5.) The temperature profile through the composite slab is also shown at several different times in Figure 6; the points on each "Finite Volume" line correspond to the cell interfaces used in the calculation (23 cells in total), and demonstrate how the technique can produce accurate results while allowing the use of non-constant cell spacing with relative ease. (Note that for simplicity the results for this TPS composite slab example assume a non-ablating/non-catalytic surface, which may not be realistic for the materials and temperatures in this example. Hence these results should be taken as a first-order thermal assessment, with additional modeling required to assess the effects due to thermochemical processes.)

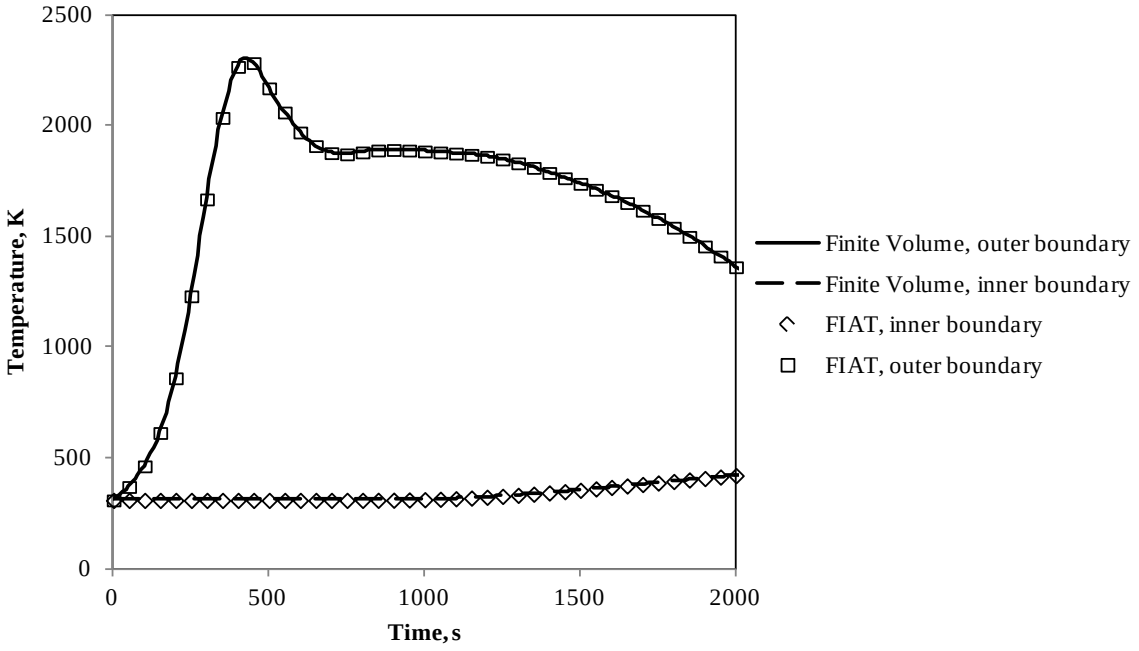

Figure 5. Thermal analysis results for TPS composite slab example.

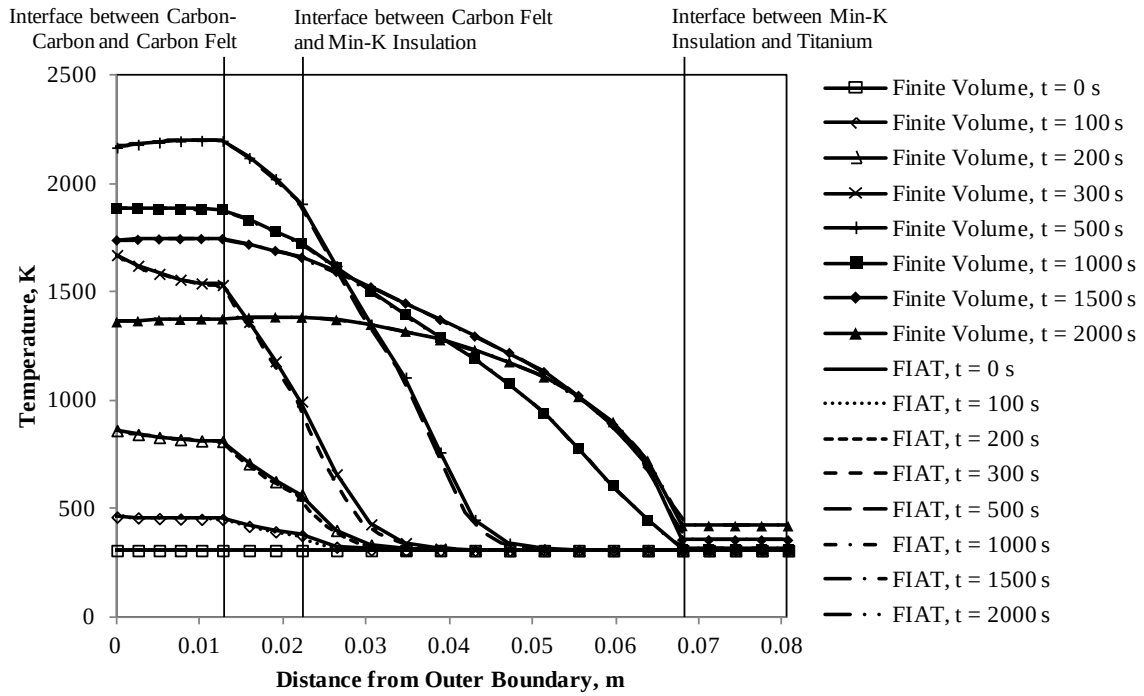

Figure 6. Temperature distribution within TPS composite slab example at different times.

6. Conclusions

The present work has outlined a finite volume approach to solving the transient one-dimensional heat diffusion equation using generalized coordinates. As demonstrated above, it can be seen how this technique can simplify the numerical solution of multi-material TPS-related engineering problems using non-uniform grid spacing. This can be useful in allowing the number of grid cells and cell spacing in each layer of a multi-material TPS analysis to be tailored to the accuracy required, with no need to maintain constant spacing throughout the material.

While beyond the scope of the present work, it should be noted that one of the advantages of deriving the finite volume solution approach from a control volume analysis is that the extension to two- and three-dimensional problems, as well as problems with non-hexahedral cells, is relatively intuitive. As equation (6) implies, the problem reduces to considering the rate of energy stored in the cell and the heat transfer across each of the cell interfaces. The present work considered heat fluxes due to conduction, convection, and radiation, but other heat fluxes (e.g., due to ablation, surface catalycity) could be added in a similar fashion. While additional dimensions introduce added complexity in the grid metrics, such as the multi-dimensional application of the chain rule of differentiation and the need to model fluxes in the three local coordinate directions for each cell face for a three-dimensional cell, standard techniques used to solve multi-dimensional fluid mechanics problems on generalized coordinates are applicable [6].

7. References

[1] Patankar, S.V., Numerical Heat Transfer and Fluid Flow, Hemisphere Publishing Corporation, 1980.

[2] Nance, D.V., "Finite Volume Algorithms for Heat Conduction," AFRL Technical Report, AFRL-RW-EG-TR-2010-049, 2010.

[3] Chen, Y.-K., and Milos, F.S., "Ablation and Thermal Response Program for Spacecraft Heatshield Analysis," *Journal of Spacecraft and Rockets*, vol. 36, no. 3, pp. 475-483, 1999.

[4] Incropera, F.P., and DeWitt, D.P., Introduction to Heat Transfer, 3rd Edition, John Wiley & Sons, Inc., 1996.

[5] Press, W.H., et al, Numerical Recipes in C, Cambridge University Press, 1997.

[6] Hoffmann, K.A., and Chiang, S.T., Computational Fluid Dynamics for Engineers – Volume I, Engineering Education System, 1993.

AEROSPACE REPORT NO.
TR-2014-01128

1-D Heat Transfer in Multilayer Materials Using a Finite Volume Approach

Approved Electronically by:

Rand H. Fisher, SR VP SPEQ
SYSTEMS PLANNING ENGINEERING & QUALITY
PRESIDENT & CEO
SYSTEMS PLANNING ENGINEERING & QUALITY

External Distribution

REPORT TITLE
1-D Heat Transfer in Multilayer Materials Using a Finite Volume Approach

REPORT NO.	PUBLICATION DATE	SECURITY CLASSIFICATION
TR-2014-01128	January 31, 2014	UNCLASSIFIED

Maj. John C. Bowman
SMC/XR
john.bowman@us.af.mil

DTIC
Defense Technical
Information Center
Distribution via AeroLibrary

Lynn Lonergan
Air University Library
lynn.lonergan@us.af.mil

NTIS
National Technical
Information Service
input@ntis.gov

APPROVED BY_____ DATE_____
(AF OFFICE) (NOT REQUIRED FOR ATR CATEGORY)